
SURVIVAEEL: Variational Autoencoders for Clustering Time Series

Anonymous Author(s)

Affiliation

Address

email

Abstract

1 Multi-state models are generalizations of time-to-event models, where individuals
2 progress through discrete states in continuous time. As opposed to classical ap-
3 proaches to survival analysis which include only alive-dead transitions, states can
4 be competing in nature and transient, enabling richer modelling of complex clinical
5 event series. Classical multi-state models, such as the Cox–Markov model, struggle
6 to capture idiosyncratic, non-linear, time dependent, or high-dimensional covari-
7 ates for which more sophisticated machine learning models are needed. Recently
8 proposed extensions can overcome these limitations, however, they do not allow for
9 uncertainty quantification of the model prediction, and typically have limited inter-
10 pretability at the individual or population level. Here, we introduce SURVIVAEEL,
11 a multi-state survival framework based on a VAE architecture, enabling uncertainty
12 quantification and interpretable patient trajectory clustering.

13 1 Introduction

14 1.1 Motivation

15 Survival analysis is of great importance in medicine with great interest in predicting the time to
16 specific events like death or adverse events, while taking into account missing outcomes due to loss
17 to follow-up. The de facto standard model in medicine today is the Cox proportional hazards (PH)
18 model [8], a semi-parametric model making strong assumptions on the functional dependence of
19 hazard rates on covariates. By now there has been a plethora of machine learning models generalizing
20 beyond the PH assumption and allowing non-linear covariate influences [16, 20, 19, 5].

21 With the rise of electronic health records there is an ever increasing amount of information available
22 and the possibility to model clinical patient trajectories in more detail, going beyond binary time-
23 to-event analysis. In many cases, disease progression or other clinical events can be modeled with
24 discrete states, e.g. tumor progression, side effects to treatments or relapse/remission after tumor
25 surgery. The default approach in this case is the Cox–Markov model, describing any possible
26 transition with a Cox-PH model without taking into account the previous disease trajectory and
27 assuming piece-wise constant hazard rates. To advance beyond these very limiting assumptions
28 SURVNODE, a machine learning model based on neural ordinary differential equations [7], has been
29 introduced by Groha et al. [12]. By using a neural network and introducing hidden states in the time
30 evolution, SURVNODE gets around the limiting assumptions of the Cox–Markov model, however, at
31 the price of losing most of its interpretability as well as a clear means of uncertainty quantification.
32 The goal of this manuscript is to add these two features, while retaining the flexibility of SURVNODE.

33 1.2 Multi-state survival analysis

34 We define a continuous time stochastic process $\{Y(t); 0 \leq t \leq T\}$ over a finite state space $Y =$
35 $\{1, \dots, S\}$, corresponding to the discrete states of the multi-state model. In the following, we will

36 briefly introduce the likelihood function and its relation to the Kolmogorov forward equations [18, 11].
 37 As the approach introduced here is an extension of SURVNODE, the presentation closely follows that
 38 of [12].
 39 For each patient, the process is observed at predefined times t_1, \dots, t_m where the patient is in states
 40 $y(t_1), \dots, y(t_m)$. The likelihood is given by

$$P(y(t_1), \dots, y(t_m) | \mathcal{H}_{t_m}; \theta) = P(y(t_1)) \prod_{j=2}^m P_{y(t_{j-1})y(t_{j-1})}(t_{j-1}, t_j | \mathcal{H}_{t_{j-1}}; \theta) \\ \times \lambda_{y(t_{j-1})y(t_j)}(t_j | \mathcal{H}_{t_j}; \theta),$$

41 where θ denotes all free model parameters, $P(y(t_1))$ the probability to be in the initial state, $P_{ij}(s, t)$
 42 the transition probability between any set of states i, j occurring at time points s, t and \mathcal{H}_t the
 43 filtration up until, but excluding time t . The full likelihood for all n patients is given by

$$\mathcal{L}(\theta; \{y_1, \dots, y_n\}) = \prod_{i=1}^n P(y_i(t_1^i), \dots, y_i(t_{m_i}^i) | \mathcal{H}_{t_{m_i}^i}; \theta),$$

44 with $y_i = \{y_i(t_1^i), \dots, y_i(t_{m_i}^i)\}$, $i = 1, \dots, n$. To accommodate censoring, the likelihood has to be
 45 adjusted. With the assumption of independent censoring, we observe $\{x_i, y_i, \delta_i; j = 1, \dots, m_i, i =$
 46 $1, \dots, n\}$, where x_i are individual covariates, m_i is the number of transitions the individual i is going
 47 through and y_i are as above or the state at time of last contact. Censoring is indicated by $\delta_i = 0$
 48 whereas we write $\delta_i = 1$ if the event is observed. The corresponding likelihood can then be written as

$$\mathcal{L}(\theta; \{y_1, \dots, y_n\}) = \prod_{i=1}^n P(y_i(t_1^i)) \prod_{j=2}^{m_i-1} P_{y_i(t_{j-1}^i)y_i(t_{j-1}^i)}(t_{j-1}^i, t_j^i; \theta) \lambda_{y_i(t_{j-1}^i)y_i(t_j^i)}(t_j^i | \theta) \\ \times P_{y_i(t_{m_i-1}^i)y_i(t_{m_i-1}^i)}(t_{m_i-1}^i, t_{m_i}^i; \theta) \left(\lambda_{y_i(t_{m_i-1}^i)y_i(t_{m_i}^i)}(t_{m_i}^i | \theta) \right)^{\delta_i},$$

49 where we omitted the dependence on the filtration for notational brevity. The evolution of the
 50 transition probabilities is governed by the Kolmogorov forward equation

$$\frac{dP_{ij}(s, t | \mathcal{H}_t)}{dt} = \sum_k P_{ik}(s, t | \mathcal{H}_t) \lambda_{kj}(t | \mathcal{H}_t), \quad i = 1, \dots, S, \quad j = 1, \dots, S, \quad (1)$$

51 which relates the intensities $\lambda_{ij}(t)$ to the transition probabilities $P_{ij}(s, t)$. Upon solving this equation
 52 we have all the ingredients for the likelihood function.

53 1.3 NeuralODE for multi-state survival modelling

54 The idea underlying SURVNODE is to model the instantaneous transition rates $\lambda_{ij}(t)$ using a neural
 55 network and solving the Kolmogorov forward equation using neural ODEs [7]. To incorporate the
 56 covariates and to include an approximation of the filtration of the process, SURVNODE introduces
 57 auxiliary memory states $m(t)$, itself modelled by an ODE

$$\frac{dm_i}{dt} = M_i(t, \mathbf{P}(t), \mathbf{m}(t)).$$

58 The initial conditions are encoded by the covariates of the patient $m(0) = f(x)$, where f is given by
 59 a neural net. This implies having to solve the system of differential equations

$$\frac{dP_{ij}(0, t)}{dt} = \sum_k P_{ik}(0, t) \lambda_{kj}(t, \mathbf{P}(0, t)(t), \mathbf{m}(t)) \\ \frac{dm_i}{dt} = M_i(t, \mathbf{P}(0, t), \mathbf{m}(t)).$$

60 Using that $P(s, 0) = P^{-1}(0, s)$ one can obtain $P_{ij}(s, t)$ at any s and t .

61 2 SURVIVAEAL

62 To obtain a quantification of model uncertainty and interpretability, we extend the model to a variational setting by introducing latent variables. Instead of maximum likelihood estimation, the objective will be the variational free energy or evidence lower bound ELBO. The variational model assumes the existence of a latent state z , which replaces the role of the initial memory state $\mathbf{m}(0)$ above, such that $\mathcal{L}(\theta; \mathcal{Y}, z)$ does not depend on the covariates x given z . A graphical representation is given in Figure to the left.

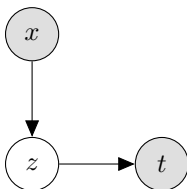


Table 1: Benchmark on the METABRIC data-set. The other models are taken from [19] and [12].

Metric	Cox-PH[8]	DeepSurv [16]	DeepHit [20]	RSF [14]	SURVNODE	SURVIVAEEL
c	0.628	0.636	0.675	0.649	0.667	0.646
ibs	0.183	0.176	0.184	0.175	0.157	0.170
inbll	0.538	0.532	0.539	0.515	0.477	0.503

63 We can derive the variational lower bound in a similar way to a (supervised) VAE [17, 15] as

$$\log p(t | x) = \log \int p(t | z)p(z | x) \geq E_{q(z|t,x)} \left[\log \frac{p(t | z)p(z | x)}{q(z | t, x)} \right].$$

64 The objective is then

$$\text{ELBO}(\theta, \mathcal{Y}) = \mathbb{E}_{q(\mathbf{z}|t,\mathbf{x})} [\log \mathcal{L}(\theta; \mathcal{Y}, \mathbf{z})] - \mathcal{D}_{KL}(q(\mathbf{z} | t, \mathbf{x}) \| p(\mathbf{z} | \mathbf{x}))$$

65 where we model the variational distribution $q(\mathbf{z}|t, \mathbf{x})$ and the prior $p(\mathbf{z}|\mathbf{x})$ as

$$q(\mathbf{z}|t, \mathbf{x}) = \mathcal{N}(\mathbf{z}; \mu_q(x, t), \text{diag}(\sigma_q^2(x, t))) \quad \text{and} \quad p(\mathbf{z}|\mathbf{x}) = \mathcal{N}(\mathbf{z}; \mu_p(x), \text{diag}(\sigma_p^2(x))),$$

66 with neural networks for μ_q , μ_p , σ_q , and σ_p , encoding the covariates into the latent space. For
 67 prediction, we obtain realizations of the transition matrix $P_{ij}(0, t)$ by repeated sampling from the
 68 prior and taking the mean as well as the 95% credible interval.

69 3 Experiments

70 3.1 Survival: benchmark of model

71 We benchmark the variational model against various survival frameworks on the METABRIC breast
 72 cancer data set [9, 24]. We compare concordance (c)[2], integrated Brier score (ibs)[4], as well as
 73 the integrated binomial log-likelihood estimator (ibll)[19] using five-fold cross validation in Table 1.
 74 SURVIVAEEL is presented with only manual hyper-parameter tuning, whereas the other models went
 75 through an extensive hyperparameter search. We still find that the model is competitive in terms of
 76 survival prediction, retaining a lot of flexibility of SURVNODE.

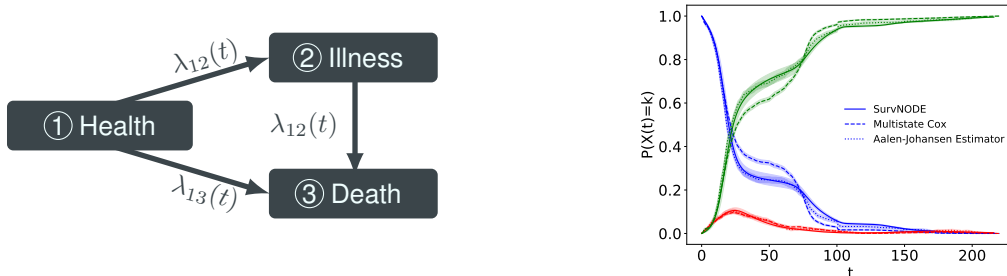


Figure 1: Left: Graphical representation of the Illness-death model. Right: Plot of probabilities for being in the different states of the illness-death model. Blue corresponds to “Health”, red to “Illness” and green to “Death”. The shaded area represents the 95% confidence intervals.

77 3.2 Multi-state survival

78 For illustration in the multi-state case, we compare performance on the population level with the
 79 non-parametric Aalen–Johansen estimator [1] for an illness-death model (see Figure 1). As a baseline,
 80 we simulate a data set with one binary covariate and proportional hazards violation using the `coxed`
 81 R package [13]. We compare our model with the standard tool in the multi-state survival literature,
 82 which is fitting a Cox proportional hazard model to each transition, treating the other events as
 83 censored [10]. The comparison can be seen in Figure 1, where we plot the predicted probabilities for
 84 the occupation of every state over time together with the non-parametric Aalen–Johansen estimator.
 85 We see a clear advantage of our model over the cause-specific Cox model and more importantly we
 86 see that the confidence intervals of SURVIVAEEL include the non-parametric estimator for most times.

Table 2: Comparison of SURVNODE and the Cox proportional hazard model in terms of calibration and concordance.

Model	calibration	concordance
Cox proportional hazards model [8]	0.250 ± 0.015	0.6244 ± 0.0064
SURVVAEL	0.749 ± 0.071	0.6396 ± 0.0097

87 **Calibration of the credible intervals** While our model captures the non-parametric estimator by
 88 visual inspection, we seek to quantify the calibration performance in simulations where the ground
 89 truth is known. We simulate a survival data set with three covariates with the `coxed` package, where
 90 we also extract the underlying individual survival probabilities. To estimate calibration of the error
 91 intervals, we therefore calculate the average of fraction of times the true survival probabilities we
 92 sample from lie within the 95% credible interval. We compare the calibration of our model to the
 93 prediction from a Cox proportional hazards model using Wald type error estimates. For one random
 94 realization of the simulated data we perform a five fold cross validation in Table 2. We find that
 95 our model produces more consistent and better calibrated error intervals than the Cox proportional
 96 hazards model, as shown in Table 2

97 **Clustering of the latent space** An additional useful feature of the latent variable model can be
 98 found by inspection of the latent space of the model. Using a simulated illness-death model with nine
 99 covariates we run the variational SURVNODE model with early stopping using a validation set and
 100 then inspect the latent on a test data-set. Using UMAP [22] we identify five clusters (Figure 2). We
 101 examine the probabilities to be in each of the three states for each cluster in the validation data set
 102 using the non-parametric Aalen–Johansen estimator. As can be seen in Figure 2, the clusters are a
 103 meaningful unsupervised differentiation between patients and capture survival differences as well as
 104 differences in transitioning to the "Illness" state well. We can additionally obtain covariate effects
 105 associated with each cluster by using logistic regression. This feature has useful applications in a
 106 clinical setting, where identification of extreme survivors to a treatment while modeling other state
 107 transitions is of particular interest.

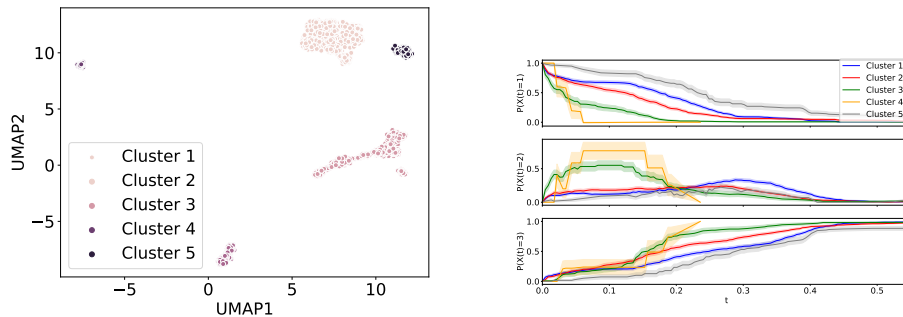


Figure 2: The latent space of the variational SURVNODE model shows meaningful clusters. The subset of patients in the clusters on the left are used in a non-parametric Aalen–Johansen estimator to obtain state occupation probabilities for all three states per cluster. The first panel is the probability for the "Health" state, the second for the "Illness" and the third for the "Death" state.

108 Our approach is directly applicable to survival analysis, where methods for example based on LDA
 109 [6] or variational inference [21] were recently proposed to cluster the latent space, but SURVVAEL
 110 generalizes those to the multi-state setting.

111 4 Conclusion

112 We have introduced a variational framework for multi-state survival analysis based on neural ODEs
 113 and shown comparable performance in the special cases of survival. Our approach allows for the
 114 estimation of credible intervals and provides an interpretability aspect, which is absent from most
 115 machine learning survival methods and the first of its kind in the setting of multi-state models.

References

- 116
- 117 [1] Odd O Aalen and Søren Johansen. An empirical transition matrix for non-homogeneous markov
118 chains based on censored observations. *Scandinavian Journal of Statistics*, pages 141–150,
119 1978.
- 120 [2] Laura Antolini, Patrizia Boracchi, and Elia Biganzoli. A time-dependent discrimination index
121 for survival data. *Statistics in medicine*, 24(24):3927–3944, 2005.
- 122 [3] Jeff Bezanson, Alan Edelman, Stefan Karpinski, and Viral B Shah. Julia: A fresh approach to
123 numerical computing. *SIAM review*, 59(1):65–98, 2017.
- 124 [4] Glenn W Brier and Roger A Allen. Verification of weather forecasts. In *Compendium of*
125 *meteorology*, pages 841–848. Springer, 1951.
- 126 [5] Paidamoyo Chapfuwa, Chenyang Tao, Chunyuan Li, Courtney Page, Benjamin Goldstein,
127 Lawrence Carin, and Ricardo Henao. Adversarial time-to-event modeling. *arXiv preprint*
128 *arXiv:1804.03184*, 2018.
- 129 [6] Paidamoyo Chapfuwa, Chunyuan Li, Nikhil Mehta, Lawrence Carin, and Ricardo Henao.
130 Survival cluster analysis. *Proceedings of the ACM Conference on Health, Inference, and*
131 *Learning*, 4 2020. doi: 10.1145/3368555.3384465.
- 132 [7] Tian Qi Chen, Yulia Rubanova, Jesse Bettencourt, and David K Duvenaud. Neural ordinary
133 differential equations. In *Advances in neural information processing systems*, pages 6571–6583,
134 2018.
- 135 [8] David R Cox. Regression models and life-tables. *Journal of the Royal Statistical Society: Series*
136 *B (Methodological)*, 34(2):187–202, 1972.
- 137 [9] Christina Curtis, Sohrab P Shah, Suet-Feung Chin, Gulisa Turashvili, Oscar M Rueda, Mark J
138 Dunning, Doug Speed, Andy G Lynch, Shamith Samarajiwa, Yinyin Yuan, et al. The genomic
139 and transcriptomic architecture of 2,000 breast tumours reveals novel subgroups. *Nature*, 486
140 (7403):346–352, 2012.
- 141 [10] Liesbeth de Wreede, Marta Fiocco, and Hein Putter. mstate: An r package for the analysis of
142 competing risks and multi-state models. *Journal of Statistical Software, Articles*, 38(7):1–30,
143 2011. ISSN 1548-7660. doi: 10.18637/jss.v038.i07.
- 144 [11] W. Feller. On the theory of stochastic processes, with particular reference to applications. In
145 *Proceedings of the [First] Berkeley Symposium on Mathematical Statistics and Probability*,
146 pages 403–432, Berkeley, Calif., 1949. University of California Press.
- 147 [12] Stefan Groha, Sebastian M Schmon, and Alexander Gusev. Neural odes for multi-state survival
148 analysis. <https://arxiv.org/abs/2006.04893>, 2020.
- 149 [13] Jeffrey J. Harden and Jonathan Kropko. Simulating duration data for the cox model. *Political*
150 *Science Research and Methods*, 7(4):921–928, 2019. doi: 10.1017/psrm.2018.19.
- 151 [14] Hemant Ishwaran, Udaya B Kogalur, Eugene H Blackstone, Michael S Lauer, et al. Random
152 survival forests. *The annals of applied statistics*, 2(3):841–860, 2008.
- 153 [15] Tom Joy, Sebastian Schmon, Philip Torr, Siddharth N, and Tom Rainforth. Capturing label
154 characteristics in VAEs. In *International Conference on Learning Representations*, 2021. URL
155 <https://openreview.net/forum?id=wQR1SUZ5V7B>.
- 156 [16] Jared L Katzman, Uri Shaham, Alexander Cloninger, Jonathan Bates, Tingting Jiang, and
157 Yuval Kluger. DeepSurv: personalized treatment recommender system using a cox proportional
158 hazards deep neural network. *BMC medical research methodology*, 18(1):24, 2018.
- 159 [17] Diederik P Kingma, Danilo J Rezende, Shakir Mohamed, and Max Welling. Semi-supervised
160 learning with deep generative models. *arXiv preprint arXiv:1406.5298*, 2014.
- 161 [18] Andrei Kolmogoroff. Über die analytischen methoden in der wahrscheinlichkeitsrechnung.
162 *Mathematische Annalen*, 104(1):415–458, 1931.
- 163 [19] Håvard Kvamme, Ørnulf Borgan, and Ida Scheel. Time-to-event prediction with neural networks
164 and cox regression. *Journal of Machine Learning Research*, 20(129):1–30, 2019.
- 165 [20] Changhee Lee, William R Zame, Jinsung Yoon, and Mihaela van der Schaar. Deephit: A deep
166 learning approach to survival analysis with competing risks. In *Thirty-Second AAAI Conference*
167 *on Artificial Intelligence*, 2018.

- 168 [21] Laura Manduchi, Ričards Marcinkevičs, Michela C Massi, Thomas Weikert, Alexander Sauter,
169 Verena Gotta, Timothy Müller, Flavio Vasella, Marian C Neidert, Marc Pfister, et al. A deep
170 variational approach to clustering survival data. *arXiv preprint arXiv:2106.05763*, 2021.
- 171 [22] Leland McInnes, John Healy, Nathaniel Saul, and Lukas Grossberger. Umap: Uniform manifold
172 approximation and projection. *The Journal of Open Source Software*, 3(29):861, 2018.
- 173 [23] Adam Paszke, Sam Gross, Francisco Massa, Adam Lerer, James Bradbury, Gregory Chanan,
174 Trevor Killeen, Zeming Lin, Natalia Gimelshein, Luca Antiga, Alban Desmaison, Andreas
175 Kopf, Edward Yang, Zachary DeVito, Martin Raison, Alykhan Tejani, Sasank Chilamkurthy,
176 Benoit Steiner, Lu Fang, Junjie Bai, and Soumith Chintala. Pytorch: An imperative style, high-
177 performance deep learning library. In H. Wallach, H. Larochelle, A. Beygelzimer, F. d'Alché-
178 Buc, E. Fox, and R. Garnett, editors, *Advances in Neural Information Processing Systems 32*,
179 pages 8024–8035. Curran Associates, Inc., 2019.
- 180 [24] Bernard Pereira, Suet-Feung Chin, Oscar M Rueda, Hans-Kristian Moen Vollan, Elena Proven-
181 zano, Helen A Bardwell, Michelle Pugh, Linda Jones, Roslin Russell, Stephen-John Sammut,
182 et al. The somatic mutation profiles of 2,433 breast cancers refine their genomic and transcrip-
183 tomic landscapes. *Nature communications*, 7(1):1–16, 2016.
- 184 [25] Christopher Rackauckas and Qing Nie. Differentialequations.jl—a performant and feature-rich
185 ecosystem for solving differential equations in julia. *Journal of Open Research Software*, 5(1),
186 2017.

187 A Implementation details

188 All models are implemented in PyTorch [23] using the `torchdiffeq` package [7]. As our example
189 networks are sufficiently small, we use backpropagation through the ODE solver to obtain gradients,
190 however, using the adjoint method is of course possible as well. We use the `dopri5` method for
191 the ODE solver with an absolute and relative tolerance of 10^{-8} in the ODE solver. To include the
192 accuracy of the solution as a hyperparameter, we scale the event times to have the maximum value
193 S , which we choose to be of $\mathcal{O}(1)$. To specify the non-zero elements of the transition rate matrix, a
194 matrix with 1 indicators for non-zero off-diagonal elements and `NaN` indicators for all other elements
195 are needed. We have the hyperparameters:

- 196 • Number of layers L_p and number of neurons per layer N_p with dropout p_p for multilayer
197 perceptron for prior $p(z|x)$;
- 198 • Number of layers L_q and number of neurons per layer N_q with dropout p_p for multilayer
199 perceptron for variational posterior $q(z|x, t)$;
- 200 • Number of layers L_Q and number of neurons per layer N_Q for multilayer perceptron
201 modeling Q ;
- 202 • Number of latent states M ;
- 203 • Coefficient of Lyapunov style loss term μ ;
- 204 • ELBO parameter β
- 205 • Scaling coefficient for event times S ;
- 206 • Learning rate l of the Adam optimizer;
- 207 • Weight decay w ,

208 where the ELBO parameter β characterizes the relative weight between log-likelihood and Kullback-
209 Leibler divergence, which we set to be 1 throughout the paper. Closer investigation of the clustering
210 property with respect to this parameter would be of interest.

211 B Clustering: Covariates and survival strata

212 To further examine the clustering of the latent space, we can superimpose the nine binary covariates
213 in the model on the UMAP projection. This can be seen in Figure 3. We see that some of the clusters
214 clearly reflect the covariates, for example in the case of covariate one, which is the lowest third of the
215 covariate with the largest effect size for one of the transitions in the simulation, we see that almost all
216 the values are in one of the clusters. By characterizing the effect of the covariates on these clusters
217 with specific survival properties, we can obtain the influence of the covariate on survival.

218 C Calibration of the credible intervals

219 A visual way to show the calibration of the credible intervals is to predict individual survival over
220 time and plot together with the true underlying survival function obtained from the `coxed` R package.
221 This can be seen in Figure 4. We see that the credible intervals contain the survival function in most
222 of the cases.

223 D Experiments

224 D.1 Simulation of data

225 The simulated data in the publication is generated in two ways. First, we simulate data with the R
226 package `coxed`.

227 In the survival cases, we choose three covariates, where one of the covariates has time varying
228 coefficients to model a proportional hazards violation. We choose all coefficients to be of $\mathcal{O}(1)$, with
229 a saw-tooth time dependence for the time dependent covariate. We sample 2048 patients for the
230 training set and 1024 patients for the validation and test set respectively with event times between
231 0 and 100. In the case of the illness death model, we sample using the `coxed` package for every
232 transition, assuming independence of each transition. We extract the covariates from the first sampled
233 model and use them for the other two survival realizations, however choosing different coefficients.

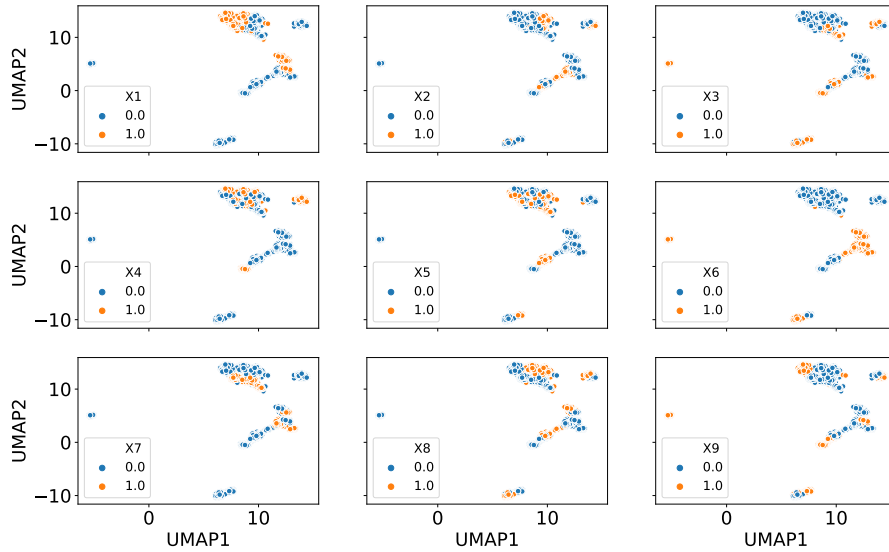


Figure 3: Possible values of the nine binary covariates in the model. We see that some of the clusters clearly reflect the covariates.

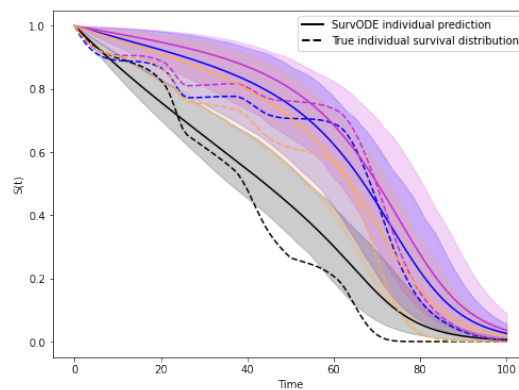


Figure 4: Predicted survival function vs real underlying survival function from the simulation. We see that the credible intervals cover the underlying survival function well.

Table 3: Characteristics of the METABRIC and SUPPORT data sets.

Data set	Size	Covariates	Unique Durations	Prop. Censored
SUPPORT	8873	14	1714	0.32
METABRIC	1904	9	1686	0.42

234 Due to a limitation of the `coxed` package, only the first sampled model can have time varying
 235 coefficients, with the other transitions then effectively being sampled from a Cox-model. In the
 236 competing case between "Illness" and "Death" from the "Health" state, we choose the first occurring
 237 time of the two sampled survival data realizations, no matter if there is censoring or not. The
 238 maximum time for the generated data in the competing case is $T = 100$, whereas we choose $T = 50$
 239 for the transition from "Illness" to "Death".

240 The second way is to directly sample from a Markov-Jump process. For this we implement a Gillespie
 241 sampling algorithm in `Julia` [3], using the `DifferentialEquations.jl` [25] package. We
 242 sample parameters for a Weibull distribution for each transition in the multi-state case and multiplica-
 243 tively add covariate dependence in a proportional hazards way. To break proportional hazards, we
 244 use time dependent coefficients for two of the 12 covariates, as in the above sampling algorithm. We
 245 choose all coefficients to be of $\mathcal{O}(1)$. We sample 5000 patients, which we then split into 64% training,
 246 16% validation and 20% test set. As we specify the underlying hazard functions, ground truth for
 247 both hazard functions as well as probability distributions is directly accessible for any multi-state
 248 model. The simulation code is available on the SURVNODE github page.

249 D.2 Data sets and hyperparameters

250 The METABRIC and SUPPORT data sets are standard survival data sets for benchmarking. The
 251 characteristics are shown in 3 [19] and are obtained from the `pycox` python package [19]. The
 252 SYNTHETIC data set in the competing hazards case is taken from [20] and available on Github with
 253 30000 patients and two outcomes, where 50% of patients experience any event, whereas the other
 254 50% are censored.

255 For all benchmark experiments we do a five-fold cross validation where we split the data in an 80 – 20
 256 split into 20% test-data and the remaining data again in an 80 – 20 split into 64% training data and
 257 16% validation data. In the comparison with the non-parametric Aalen-Johansen estimator we used

- 258 • $L_p = 2$ with $N_p = 400$ and $p_p = 0.$;
- 259 • $L_q = 2$ with $N_p = 1000$ and $p_p = 0.$;
- 260 • $L_Q = 3$ with $N_Q = 1000$
- 261 • $M = 70$;
- 262 • $\mu = 10^{-4}$;
- 263 • $S = 1.$;
- 264 • $l = 1e - 4$;
- 265 • $w = 1e - 7$;
- 266 • $\beta = 1,$

267 and for clustering the latent space the hyperparameter setting we use is

- 268 • $L_p = 2$ with $N_p = 400$ and $p_p = 0.$;
- 269 • $L_q = 2$ with $N_p = 400$ and $p_p = 0.$;
- 270 • $L_Q = 2$ with $N_Q = 1000$
- 271 • $M = 50$;
- 272 • $\mu = 10^{-4}$;
- 273 • $S = 1.$;
- 274 • $l = 5e - 5$;
- 275 • $w = 1e - 7$;
- 276 • $\beta = 1.$

277 all of which were only manually hyperparameter tuned on train and validation set.